applied sciences

MDPI

Article

Efficacy Confirmation Test of Immature Asian Pear (*Pyrus pyrifolia* Nakai) Extract on Ovalbumin-Induced Asthma in Mice

Mi Ran Kim [1,†], Khawaja Muhammad Imran Bashir [2,†], Jin-Hwa Lee [1], Mo-Un Ku [3], Joo Wan Kim [4], Ki-Young Kim [5], Su Shin [5], Eun-Jin Hong [5], Sae-Kwang Ku [6,*] and Jae-Suk Choi [1,*]

[1] Department of Seafood Science and Technology, The Institute of Marine Industry, Gyeongsang National University, Tongyeong 53064, Republic of Korea; 210217@gnu.ac.kr (M.R.K.); evolution_5237@naver.com (J.-H.L.)
[2] German Engineering Research Center for Life Science Technologies in Medicine and Environment, Busan 46742, Republic of Korea; imran.bashir@lstme.org
[3] Department of Biomedical Laboratory Science, College of Health and Welfare, Kyungwoon University, Gumi 39160, Republic of Korea; 202121018@ikw.ac.kr
[4] Department of Companion Animal Health, Daegu Haany University, Gyeongsan 38610, Republic of Korea; dvm_jkkim@dhu.ac.kr
[5] Research Institute, Bio Port Korea Inc., Busan 46034, Republic of Korea; kyk1967@bioportkorea.com (K.-Y.K.); sshin@bioportkorea.com (S.S.); ejhong@bioportkorea.com (E.-J.H.)
[6] Department of Anatomy and Histology, College of Korean Medicine, Daegu Haany University, Gyeongsan 38610, Republic of Korea
* Correspondence: gucci200@dhu.ac.kr (S.-K.K.); jsc1008@gnu.ac.kr (J.-S.C.); Tel.: +82-53-819-1549 (S.-K.K.); +82-55-772-9142 (J.-S.C.)
† These authors contributed equally to this work.

Abstract: Allergic asthma is a chronic inflammatory disease characterized by the infiltration of leukocytes, particularly eosinophils, into the airways, resulting in respiratory dysfunction. To develop new asthma treatment materials with minimal side effects and excellent bioactivities, we evaluated the efficacy of immature Asian pear extract (IAP extract; 400–100 mg/kg) in alleviating ovalbumin (OVA)-induced asthma in female C57BL/6J mice. This study assesses various parameters associated with OVA-induced allergic asthma including lung weight, macroscopic necropsy findings, the total cell count in bronchoalveolar lavage fluid (BALF), the total leukocyte count and leukocyte differential count, serum ovalbumin-specific Ig E (OVA-sIg E) levels, interleukin (IL)-4 and IL-5 contents in BALF, histopathological changes in the lungs, and alterations in oxidative stress and inflammation-related mRNA expressions. The results of this study demonstrate clear asthma-related findings in the OVA control group. However, the oral administration of IAP extract (at doses ranging from 400 to 100 mg/kg) significantly suppressed the anti-inflammatory and antioxidant activities by regulating the expressions of phosphoinositide 3-kinase/protein kinase B/phosphatase and TENsin homolog deleted on chromosome 10 (PI3K/Akt/PTEN), p38 mitogen-activated protein kinase (p38 MAPK), and nuclear factor kappa-light-chain-enhancer of activated B cells (NF-κB) in a dose-dependent manner. These effects are comparable to those observed with dexamethasone at a concentration of 0.75 mg/kg. As a result, the oral administration of an appropriate dose of IAP extract holds promise as a potential natural drug or health-functional food material for improving respiratory function.

Keywords: Asian pears; asthma; functional food; in vivo; *Pyrus pyrifolia* Nakai

Citation: Kim, M.R.; Bashir, K.M.I.; Lee, J.-H.; Ku, M.-U.; Kim, J.W.; Kim, K.-Y.; Shin, S.; Hong, E.-J.; Ku, S.-K.; Choi, J.-S. Efficacy Confirmation Test of Immature Asian Pear (*Pyrus pyrifolia* Nakai) Extract on Ovalbumin-Induced Asthma in Mice. *Appl. Sci.* **2023**, *13*, 9342. https://doi.org/10.3390/app13169342

Academic Editor: Anna Lante

Received: 31 May 2023
Revised: 11 August 2023
Accepted: 14 August 2023
Published: 17 August 2023

1. Introduction

Allergic asthma is a chronic inflammatory respiratory disease characterized by hypersensitivity of the respiratory tract to various allergens and irritants [1]. It is marked by the infiltration of eosinophils into the airways, leading to bronchiolar constriction,

increased airway hyperresponsiveness, excessive mucus production, and elevated immunoglobulin E (IgE) levels, along with significant goblet cell hyperplasia [2,3]. The global prevalence of allergic asthma has been rising, particularly in developing countries with higher levels of air pollution [4]. The key signaling pathways implicated in allergic asthma include nuclear factor kappa-light-chain-enhancer of activated B cells (NF-κB), phosphoinositide 3-kinase/protein kinase B (PI3K/Akt), and p38 mitogen-activated protein kinases (MAPK) [5–7]. Additionally, Type 2 helper T (Th2) cells and related cytokines like interleukin (IL)-4, IL-5, and IL-13 play a crucial role in asthma pathogenesis [8–10]. Among these, IL-4 is responsible for driving allergic inflammation and airway remodeling by promoting the differentiation of IgE-producing B lymphocytes [11,12]. IL-5, on the other hand, is specific to eosinophilic leukocytes and plays a critical role in their proliferation, differentiation, migration, activity, recruitment, and survival [13]. The accumulation of eosinophilic leukocytes in tissue contributes to various allergic reactions, including asthma [14]. As a result, the regulation of IL-4 or IL-5 has emerged as a significant target in the development of therapeutic agents for allergic asthma [15,16].

Currently, the most commonly employed treatments for asthma involve the inhalation of β2 receptor agonists or the inhalation and oral administration of glucocorticosteroids. However, their prolonged usage is constrained by the fact that they fail to address the root cause of asthma and are associated with diverse side effects [17]. Consequently, there exists a compelling need to formulate novel asthma treatment options that exhibit a comparatively reduced incidence of side effects while delivering heightened efficacy [18]. Within the realm of corticosteroids, dexamethasone (DEXA) stands out as one of the extensively utilized benchmark drugs in the progression of new asthma therapies [19–22]. Therefore, this study employs DEXA (0.75 mg/kg) as a control substance. This selection has been reported by a wide array of respiratory disease models available for evaluating drug efficacy, including allergic asthma [20–23].

The ovalbumin (OVA) sensitization and re-exposure (boosting) induced C57BL/6 mouse asthma model ranks among the extensively employed experimental animal models for assessing the effectiveness of asthma treatment candidates. This model is preferred due to its capability to induce distinct allergic asthmatic symptoms in animals within a mere three days subsequent to the topical re-exposure to OVA [20,21,24]. Through the utilization of this animal model, drug efficacy has primarily been gauged by monitoring alterations in the lung weight, the levels of inflammatory cytokines in lung tissue and the bloodstream, and the presence of cellular components like eosinophils and neutrophils within the bronchoalveolar lavage fluid (BALF). Additionally, a histopathological examination of the airways, encompassing the lungs, constitutes an essential aspect of this evaluation process [20,21,24].

Bioactive compounds derived from natural sources are renowned for their ability to elicit relatively low side effects while demonstrating exceptional anti-inflammatory and antioxidant properties [25,26]. Consequently, the development of respiratory protective drugs using natural substances within diverse asthma experimental animal models, including OVA-induced C57BL/6 mice, is currently advancing [20–22]. Among the spectrum of natural products, pears (*Pyrus* spp.) stand out as one of the most frequently consumed fruits worldwide [27]. In Korea, Asian pears (*Pyrus pyrifolia* Nakai) hold a prominent place as extensively cultivated oriental pear varieties [28]. A multitude of chemical compounds, including phenylpropanoid malate derivatives [28], caffeoyl triterpenes [29], and various phenolic compounds, including flavonoids, have been successfully isolated and identified as major bioactive constituents within *P. pyrifolia* [30–33]. The content of key components like the total caffeic acid, chlorogenic acid, arbutin, total phenolic compounds, malaxinic acid, and total flavonoids, which collectively constitute the primary ingredients within pears, diminishes during fruit maturation and ripening [34]. Therefore, phenolic compounds and antioxidant activity are significantly more pronounced in immature pears compared to their mature counterparts [35]. Considering the annual pear production in Korea [36], a substantial amount of thinned out superfluous fruits and immature pears,

approximately 15,000 tons per year [35], are completely discarded as waste [35]. It is noteworthy that the alcohol detoxification properties and hangover relief effects of *P. pyrifolia* have been extensively documented [37,38]. This contest highlights the strong potential for isolating physiologically active components from immature pears and their subsequent utilization in the development of functional food materials [35].

While the pharmacological benefits of Asian pears have been documented in relation to various ailments, it is worth noting that, to the best of our current understanding, the potential lung-function-improving effects of immature Asian pear extract (IAP extract) within the context of an OVA-induced mouse asthma model remain unexplored. Consequently, in pursuit of the development of potential solutions for enhancing respiratory functions, whether in the form of health-promoting functional food materials or naturally derived new drugs, this study endeavors to assess the dose-dependent impact of IAP extract on ameliorating lung impairment. To achieve this objective, an OVA-induced C57BL/6 mouse asthma model was employed, drawing upon well-established methodologies [20,21,24].

2. Materials and Methods

2.1. Test Material

Immature Asian pear extract (IAP extract; *P. pyrifolia* Nakai cv. Shingo) was procured from Bioport Korea Inc., Yangsan, Republic of Korea. The IAP powdered extract, characterized by its light brown color, exhibited solubility of up to 40 mg/mL in distilled water. The powdered extract was stored at a temperature of −20 °C for subsequent utilization. A portion of the IAP powdered extract was cataloged and stored as a specimen within the herbarium of the Medical Research Center for Herbal Convergence on Liver Disease, Daegu Haany University, Gyeongsan, Republic of Korea, under the designation of sample no. IAP2022BPK01. For the purpose of comparison, DEXA at a concentration of 0.75 mg/kg (Sigma-Aldrich, St. Louise, MO, USA) was used as a reference drug, as reported by previous studies [21–23,39].

2.2. HPLC Analyses

The quantification of arbutin within the IAP extract was performed utilizing an Agilent HPLC-1200 series instrument, which was equipped with a variable wavelength detector (Agilent Technologies, Inc., Santa Clara, CA, USA). This analysis was conducted employing a Capcell Pak C18 UG120 column (4.6 mm × 250 mm, 5 µm; Osaka Soda Co. Ltd., Osaka, Japan). The IAP extract, alongside standard arbutin (L14945; Alfa Aesar, Ward Hill, MA, USA), was dissolved within a mobile phase solvent. The solvent comprised a mixture of 10 mM monopotassium phosphate (KH_2PO_4) and acetonitrile at a ratio of 98.9:1.1, respectively. The HPLC samples were filtered through 0.45 µm membrane filters. During the course of analysis, the column was maintained at a consistent temperature of 30 °C and the sample assessment was performed at 280 nm. A sample volume of 10 µL was injected at a flow rate of 0.8 mL/min. Subsequently, the resulting data were quantified by comparison with the established standard arbutin.

2.3. Laboratory Animals

A total of 66 six-week-old SPF/VAF inbred (C57BL/6JBomTac) female mice from Daehan Bio Link, Eumseong, Republic of Korea, were acclimatized for seven days at laboratory conditions characterized by a temperature range of 20–25 °C, humidity levels of 30–35%, and a 12:12 h light–dark cycle. After one week of rearing the experimental animals, only those displaying consistent body weight gains and exhibiting behavioral abnormalities on the functional observational battery test were selected and included in this study. For proper grouping, the mice were categorized based on their measured average body weights, which were as follows: intact vehicle control group (16.91 ± 0.51 g) and OVA-induced asthma test group (16.90 ± 0.56 g). This categorization was performed one day before the initiation of the first sensitization and the initial administration of the test substance. Asthma was induced through intraperitoneal (IP) injection of a 10 mg OVA

solution (A5503; Sigma-Aldrich). Notably, a prior study involving Asian pear extract [40] revealed that female C57BL/6J mice were more susceptible to $PM_{2.5}$-induced lung damage, with their neonatal offspring also demonstrating toxicity upon $PM_{2.5}$ exposure during pregnancy. Similar trends were also observed by Chen et al. [41] and Guo et al. [42], thus leading us to anticipate a parallel trend in the present study. Furthermore, it is important to note that female mice were chosen as the experimental animal model in this study due to their suitability for group life, docile nature, relatively lower weight compared to males, and ease of handling. These factors collectively contribute to the practicality of using female C57BL/6J mice for this experimental investigation.

A total of six animal groups were included in this study, each consisting of ten animals (n = 10). The animal experiments were conducted under the prior approval of the Animal Experiment Ethics Committee of Daegu Haany University (approval no. DHU2022-120; approved on 20 December 2022). All experimental animals underwent an 18 h fasting period prior to the initiation of test substance administration (first sensitization by OVA) and the final necropsy day. Importantly, it should be noted that access of drinking water remained unrestricted for the duration of this fasting period.

The experimental animals were categorized into the following test groups:

1. Intact vehicle control: Vehicle-treated normal control mice;
2. OVA control: OVA-sensitized and boosted mice with oral administration of vehicle;
3. DEXA: OVA-sensitized and boosted mice with oral administration of 0.75 mg/kg of DEXA;
4. IAP_{400}: OVA-sensitized and boosted mice with oral administration of 400 mg/kg of IAP extract;
5. IAP_{200}: OVA-sensitized and boosted mice with oral administration of 200 mg/kg of IAP extract;
6. IAP_{100}: OVA-sensitized and boosted mice with oral administration of 100 mg/kg of IAP extract.

2.4. Induction of Asthma

The laboratory animals were sensitized following well-established procedures [20,21,24]. Briefly, the sensitization process involved the IP injection of a solution comprising 10 mL/kg of a 10 mg OVA solution that was saturated in 20 mL of physiological saline solution containing 0.9 mg of aluminum hydroxide ($Al(OH)_3$; A8222; Sigma-Aldrich). This injection was administered into the lower right abdomen of the experimental animals, and the sensitization was repeated twice with a 7-day interval between administrations. Subsequent to the final sensitization, asthma induction was achieved through a process of re-exposure (boosting). This involved the nasal cavity application of an OVA solution (10 µg of OVA dissolved in 50 µL of physiological saline) twice daily for a continuous period of 2 days (resulting in a total of 4 exposures).

To ensure uniform calibration and dosing across the intact vehicle control group, a parallel approach was taken. During sensitization, an $Al(OH)_3$ solution was administered via IP injection at the same dose. In the context of boosting, only physiological saline (without OVA) was introduced into the nasal cavity, adhering to the same dosing and administration procedure.

2.5. Administration of Test Material

The IAP extract, the test material, was dissolved in sterile distilled water at concentrations of 40, 20, and 10 mg/mL. These solutions were orally administered to the experimental animals via gastric gavages once daily at a dose of 10 mL/kg (subsequent final concentrations of 400, 200, and 100 mg/kg) for 16 days. The IAP extract dosages of 400, 200, and 100 mg/kg and the treatment duration were selected based on a prior study involving Asian pear extract [40]. In parallel, DEXA (Sigma-Aldrich) was also dissolved in sterile distilled water at a concentration of 0.075 mg/mL and was orally administered once daily for 16 days, with each animal receiving 10 mL/kg, corresponding to a dosage of

0.75 mg/kg [21–23,39,43,44]. To ensure consistent handling, restraint, and administration stress, the control groups underwent the same process. However, instead of the test substance or DEXA, these control groups received oral administration of sterile distilled water as a vehicle.

2.6. Removal of Lung Tissue

Twenty-four hours after the 16th administration of the test material, a comprehensive lung examination was conducted. This involved the removal of the entire lung from each experimental animal, followed by a measurement of its total weight using an automatic scale (XB320M; Precisa Instrument, Dietikon, Switzerland). The left secondary bronchus and the right lower lobe secondary bronchus were ligated using sterilized 3-0 nylon thread (NB 324; AILEE, Busan, Republic of Korea). The left lobe of the lung was utilized for both gross and histopathological observation, and the middle lobe and right upper lobe were used for BALF collection, facilitating the extraction of important biological material for analysis. Additionally, the right lower lobe was reserved for reverse transcription polymerase chain reaction (RT-PCR) analysis, which focused on examining gene expression patterns related to NF-κB, p38 MAPK, phosphatase, and TENsin homolog deleted on chromosome 10 (PTEN), Akt, and PI3K.

2.7. Observation Items

Body weight, weight gain, lung weight, gross autopsy finding, total cell counts in BALF, total leukocyte counts and leukocyte fraction counts, OVA-sIg E content in serum, IL-4 and IL-5 contents in lung tissue, BALF and IL-5 contents, histopathological changes in lungs, and changes in oxidative stress and inflammation-related gene expressions were evaluated using a CFX96TM Real-Time PCR System (Bio-Rad, Hercules, CA, USA). These parameters were investigated based on methods that were previously established in our earlier studies [20,21,45]. Each method is briefly described below.

2.7.1. Body Weight and Weight Gain

Variations in body weight and weight gain were meticulously tracked throughout the study timeline using an electronic scale (Precisa Instrument). The measurements were recorded at one day prior to the commencement of the initial test material administration, on the day of the first test material administration, and at intervals of 1, 7, 14, 15, and 16 days following the initiation of the test material administration. To minimize the potential influence of feed intake on weight deviation, fasting was implemented on both the day before and the final day of test material administration.

2.7.2. Lung Gross Necropsy Findings

After the lungs were separated and weighed, two 3-0 nylon ligations (AILEE) were performed on the left secondary bronchus and the right lower secondary bronchus. The left lung was used for both gross and histopathological evaluations. The middle and right upper lobes of the lung were used for BALF collection, and the right lower lobes of the lung were preserved for subsequent analyses involving cytokines and mRNA expression. Furthermore, the acquired gross digital images of individual lungs were subject to calculation to determine the percentage of congestion regions using a computer-assisted automated image analyzer (iSolution FL, ver. 9.1, IMT i-solution Inc., Bernaby, BC, Canada).

2.7.3. BALF Leukocyte Fractionation

BALF was collected from the bloodstream by following the protocol established by Glynos et al. [46]. Subsequently, an automatic cell counter (Countess C10281; Invitrogen, Carlsbad, CA, USA) was used to perform a comprehensive analysis of cellular constituents present within the BALF. The number of various types of white blood cells, including lymphocytes, neutrophils, acid neutrophils, and monocytes were analyzed in accordance using the previously established protocol of Shu et al. [47].

2.7.4. Histopathological Changes in Lung Tissue

The left lobe was fixed in 10% neutral buffered formalin for 24 h. Subsequently, paraffin blocks were employed to prepare tissue slides using an automatic microtome (RM2255; Leica Biosystems, Nussloch, Germany). The prepared tissue slides were stained with hematoxylin and eosin (H&E; Sigma-Aldrich) for general histopathology, toluidine blue (TB; Sigma-Aldrich) for mast cells, and Congo red (CR; Sigma-Aldrich) for eosinophils, as reported in the previously established protocols [20,21]. The stained tissue sections were then subjected to histomorphometrical analysis, utilizing a computer-based image analysis program and camera system (iSolution). The studied parameters included the mean alveolar septal thickness (μm), the mean alveolar surface area (ASA; %/mm^2) reflected by the pulmonary functions' gas exchange capacities [21,39,40], the number of PAS-positive mucus-producing cells on the secondary bronchus, and the number of inflammatory cells in the alveolar regions (cells/mm^2) [21,39,40]. The selection of histological fields for inspection was consistent, with the upper regions of the secondary bronchus being chosen. A minimum of one field from each tissue of the left lung was selected, amounting to a total of ten histological lung fields per group.

2.7.5. mRNA Expression in Lung Tissue

In lung tissue, the assessment of the mRNA expression levels for genes related to oxidative stress (NF-κB, p38 MAPK, PTEN, PI3K, and Akt) and inflammation (IL-4 and IL-5) was conducted using established methods, as demonstrated by Deng et al. [48] and Duong et al. [49]. The primer pairs were synthesized from OriGene Technologies (Rockville, MD, USA), and the specific oligonucleotides employed in this study are detailed in Table S1. Briefly, the procedural steps were as follows: RNA was extracted using Trizol reagent (15596018; Invitrogen, Carlsbad, CA, USA) and the extracted RNA was treated with recombinant DNase I (AM1906; DNA-free DNA Removal Kit; Thermo Fisher Scientific Inc., Rockford, IL, USA) to remove DNA contamination. A High-Capacity cDNA Reverse Transcription Kit (4368813; Thermo Fisher Scientific Inc.) was utilized for the reverse transcription of RNA, adhering to the manufacturer's instructions. A real-time PCR analysis was performed using the Bio-Rad real-time system (Bio-Rad). The thermal cycle conditions consisted of multiple steps: activation at 50 °C for 2 min, pre-soaking at 95 °C for 10 min, denaturation at 95 °C for 15 s, annealing at 60 °C for 1 min, and a melting curve process involving cycles of 95 °C for 15 s, 60 °C for 15 s, and 95 °C for 15 s. The acquired data were normalized using β-actin (Actb) mRNA expression as a reference. The expression patterns were quantified using the comparative threshold cycle ($2^{-\Delta\Delta Cq}$) method of Schmittgen and Livak [50].

2.8. Statistical Analysis

All reported values are presented as means and standard deviations (S.D.) derived from a sample size of ten mice within each experimental group (n = 10). The statistical significance between these groups was undertaken through a one-way analysis of variance (ANOVA) test using the SPSS ver. 18 (SPSS Inc., Chicago, IL, USA). The assessment of variance homogeneity was conducted using the Levene test. In situations where no significant differences were observed, a subsequent verification of significance was performed using Tukey's honest significant difference (THSD) test. However, if a significant deviation was identified in the Levene test, the significance was instead verified using Dunnett's T3 (DT3) test, as previously demonstrated in our earlier studies [20,21,45].

3. Results

3.1. Arbutin Content in IAP Extract

An HPLC analysis of the IAP extract revealed the presence of arbutin at a concentration of 9.10 mg/g (Figure S1).

3.2. Changes in Body Weight

At the fourteen days after the initial administration of the test substance, a statistically significant weight loss ($p < 0.01$) was observed in the group administered with DEXA in comparison to the intact vehicle control group. During the course of the experimental period, there was a significant reduction in weight gains as well. Conversely, no significant changes in body weights and weight gains were evident in any of the groups with OVA-induced asthma. Furthermore, at the seventh day after the initial administration, a significant weight loss ($p < 0.01$) was observed in the DEXA-administered group, and there was a noteworthy decrease ($p < 0.05$) in weight gain as compared to the OVA control group. Notably, no significant changes in body weights or weight gains were recorded among the groups administered with different doses of IAP extract in comparison to the OVA control group (Figure 1 and Table S2).

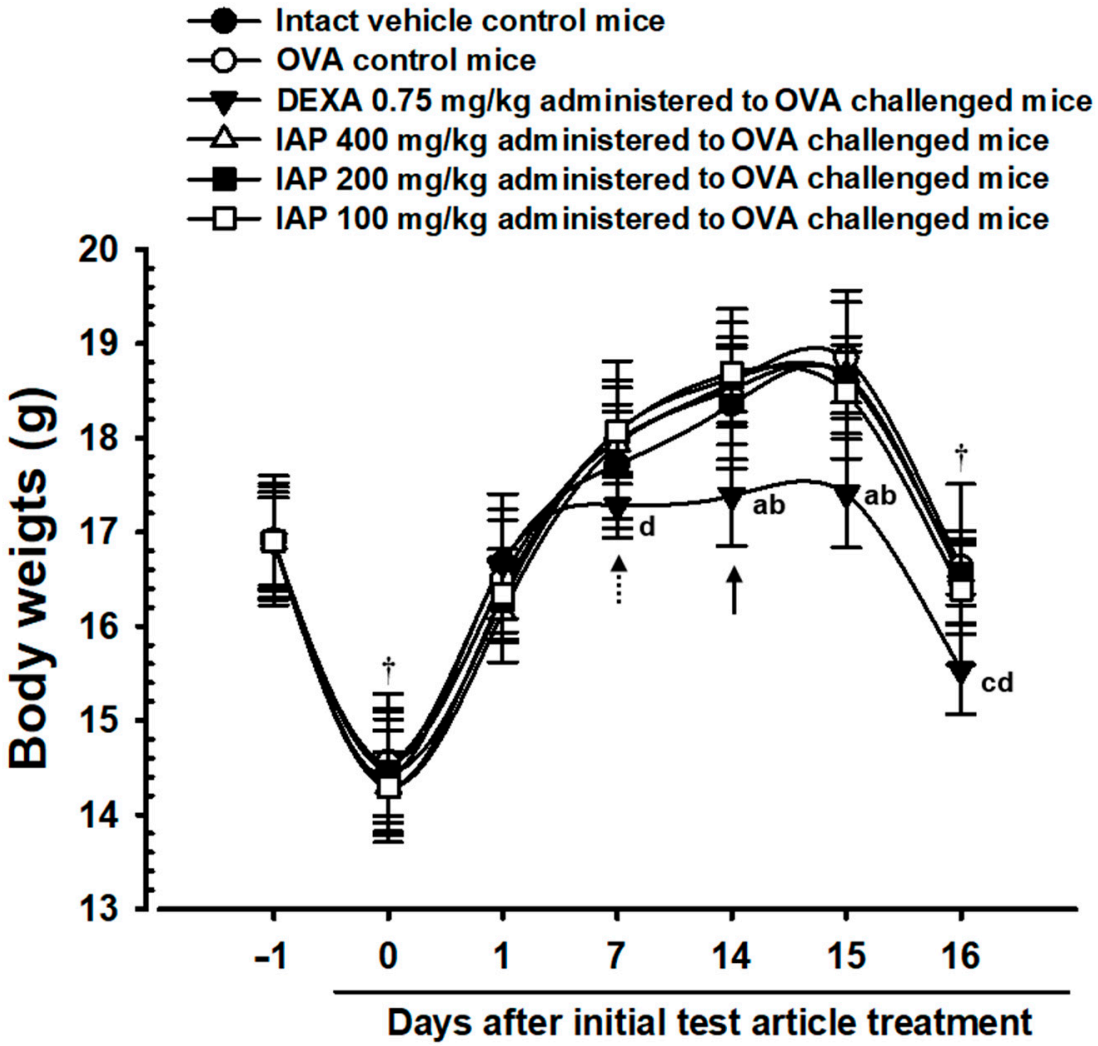

Figure 1. Changes in body weight in intact or OVA-induced allergic asthma mice. Arrow indicates significant ($p < 0.01$) decreases in body weights in DEXA-administered mice 14 days after initial oral administration. Dotted arrow indicates significant ($p < 0.01$) decreases in body weights in DEXA-administered mice 7 days after initial oral administration. All animals were fasted overnight before initial test material administration and sacrifice (†). [a] $p < 0.01$ compared with intact vehicle control using THSD test; [b] $p < 0.01$ compared with OVA control using THSD test; [c] $p < 0.01$ compared with intact vehicle control using DT3 test; [d] $p < 0.01$ compared with OVA control using DT3 test.

3.3. Lung Gross Necropsy Findings and Changes in Lung Weight

The OVA control group showed evident lung enlargement coupled with pronounced local congestion. This was substantiated by a significant ($p < 0.01$) augmentation in the visually assessed congestion area, as well as the absolute and relative lung weights, when contrasted with the intact vehicle control group. In contrast, significant ($p < 0.01$) decreases in the gross lung congestion, as well as the absolute and relative lung weights, were distinctly observed in all three doses of IAP-extract-administered groups, following a dose-dependent pattern. In particular, the IAP_{400} group demonstrated a remarkable inhibitory effect against OVA-induced lung congestion, enlargement, and an increase in absolute and relative lung weights. This was comparable to that exhibited by the DEXA-administered group (Figure 2 and Table S3).

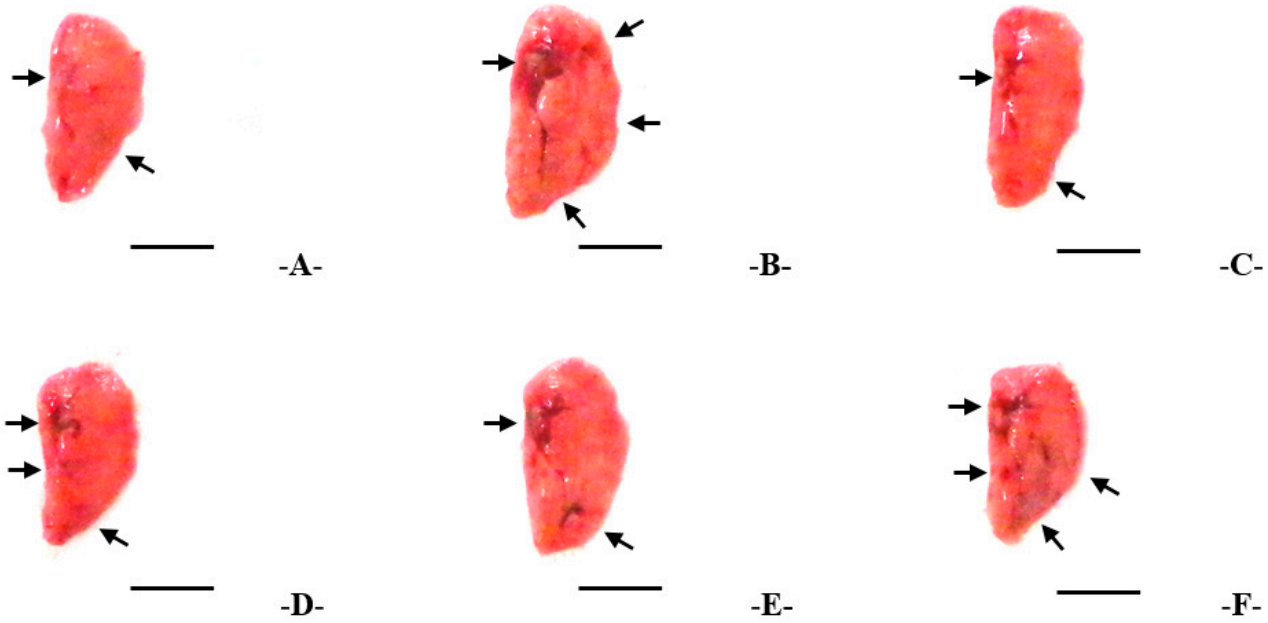

Figure 2. Representative gross lung—left lobe images taken from intact or OVA-induced allergic asthma mice. (**A**) Vehicle-treated normal control mice (intact vehicle control); (**B**) OVA-sensitized and boosted mice with oral administration of vehicle (OVA control); (**C**) OVA-sensitized and boosted mice with oral administration of 0.75 mg/kg of DEXA (DEXA); (**D**) OVA-sensitized and boosted mice with oral administration of 400 mg/kg of IAP extract (IAP_{400}); (**E**) OVA-sensitized and boosted mice with oral administration of 200 mg/kg of IAP extract (IAP_{200}); (**F**) OVA-sensitized and boosted mice with oral administration of 100 mg/kg of IAP extract (IAP_{100}). Arrows indicate congestional regions. Scale bars: 5.00 mm.

3.4. Changes in Total Cell Count, Total Leukocyte Count, and Leukocyte Count in BALF

In the OVA control group, a statistically significant ($p < 0.01$) increase in the counts of total cells, total leukocytes, lymphocytes, neutrophils, coral leukocytes, and monocytes within the BALF was evident when compared to the intact vehicle control group. In a contrasting pattern, substantial reductions ($p < 0.01$; $p < 0.05$) in the counts of total cells, total leukocytes, lymphocytes, neutrophils, coral leukocytes, and monocytes in the BALF were consistently observed across all three doses of IAP-extract-administered groups, following a dose-dependent trend. In particular, the IAP_{400} group exhibited significant inhibition of the increase in total cells and leukocytes counts within OVA-induced BALF, and a comparable response was observed in the DEXA-treated group (Table 1).

Table 1. Cytology of BALF in intact or OVA-induced allergic asthma mice.

Groups	Total Cells	Total Leukocytes	Differential Counts			
			Lymphocytes	Neutrophils	Eosinophils	Monocytes
Controls						
Intact vehicle	15.00 ± 1.94	10.60 ± 2.01	6.90 ± 1.60	2.20 ± 0.79	0.21 ± 0.19	0.21 ± 0.13
OVA	57.80 ± 3.55 [a]	51.50 ± 3.47 [c]	32.00 ± 3.74 [a]	11.40 ± 1.26 [c]	2.99 ± 0.80 [c]	3.12 ± 0.79 [c]
Reference						
DEXA	25.30 ± 4.14 [ab]	20.10 ± 2.73 [ce]	12.10 ± 1.52 [ab]	4.80 ± 2.10 [de]	0.81 ± 0.27 [ce]	0.87 ± 0.19 [ce]
Test material groups						
IAP_{400}	25.60 ± 3.50 [ab]	20.60 ± 3.60 [ce]	12.30 ± 1.64 [ab]	4.90 ± 1.66 [ce]	0.84 ± 0.32 [ce]	0.89 ± 0.31 [ce]
IAP_{200}	33.40 ± 5.27 [ab]	27.00 ± 4.71 [ce]	16.50 ± 3.03 [ab]	6.20 ± 1.55 [ce]	1.33 ± 0.33 [ce]	1.69 ± 0.40 [ce]
IAP_{100}	42.30 ± 4.24 [ab]	34.80 ± 2.49 [ce]	21.40 ± 2.46 [ab]	7.60 ± 1.17 [ce]	1.64 ± 0.22 [ce]	2.12 ± 0.21 [cf]

Cell number: 1×10^4 cells/mL. [a] $p < 0.01$ compared with intact vehicle control using THSD test; [b] $p < 0.01$ compared with OVA control using THSD test; [c] $p < 0.01$ and [d] $p < 0.05$ compared with intact vehicle control using DT3 test; [e] $p < 0.01$ and [f] $p < 0.05$ compared with OVA control using DT3 test.

3.5. Changes in Serum OVA-sIg E Content

Within the OVA control group, a statistically significant augmentation ($p < 0.01$) in the content of serum OVA-sIg E was evident when contrasted with the intact vehicle control group. In contrast, a significant and consistent decline ($p < 0.01$) in the serum OVA-sIg E content was distinctly observed across all three doses of the IAP-extract-administered groups, in accordance with a dose-dependent pattern. In particular, the IAP_{400} group exhibited an inhibitory effect against the OVA-induced increase in the serum OVA-sIg E content, which is a response that is comparable to that elicited by the DEXA-administered group (Figure 3).

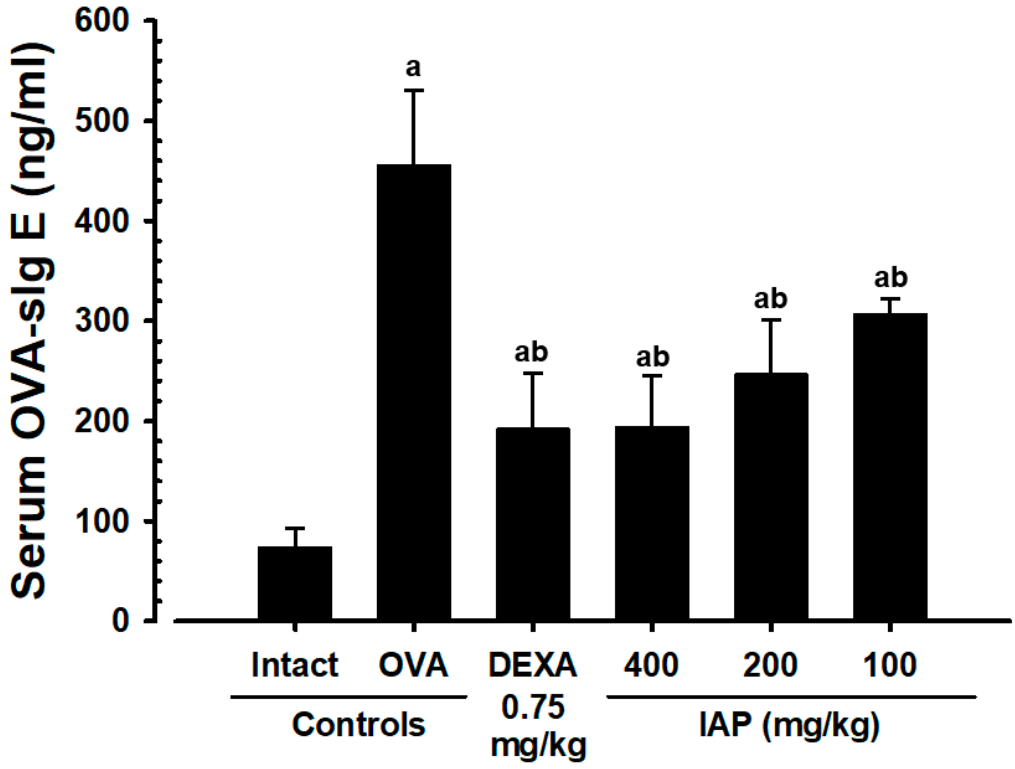

Figure 3. Serum OVA-sIg E levels in intact or OVA-induced allergic asthma mice. [a] $p < 0.01$ compared with intact vehicle control using DT3 test; [b] $p < 0.01$ compared with OVA control using DT3 test.

3.6. Changes in Cytokine IL-4 and IL-5 Contents in BALF and Lung Tissue

Within the OVA control group, a statistically significant increase ($p < 0.01$) in the levels of cytokine IL-4 and IL-5 was observed in both the BALF and lung tissue compared to the intact vehicle control group. In contrast, a significant and dose-dependent decrease ($p < 0.01$) in the contents of IL-4 and IL-5 within both the BALF and lung tissue was evident across all three doses of IAP-extract-administered groups. In particular, the IAP_{400} group exhibited an inhibitory effect against the OVA-induced surge in the IL-4 and IL-5 levels within the BALF and lung tissue, which is a response that is comparable to that observed of the DEXA-administered group (Table 2).

Table 2. BALF and lung tissue cytokine (IL-4 and IL-5) contents in intact or OVA-induced allergic asthma mice.

Groups	BALF Contents (pg/mL)		Lung Tissue Contents (pg/mL)	
	IL-4	IL-5	IL-4	IL-5
Controls				
Intact vehicle	18.80 ± 4.24	21.00 ± 6.22	39.70 ± 11.53	44.90 ± 12.85
OVA	98.70 ± 12.53 [a]	148.30 ± 12.65 [a]	158.50 ± 18.78 [a]	174.80 ± 23.38 [a]
Reference				
DEXA	35.60 ± 12.75 [bc]	59.80 ± 14.56 [ac]	62.30 ± 14.45 [bc]	78.40 ± 19.73 [ac]
Test material groups				
IAP_{400}	36.20 ± 10.77 [bc]	60.60 ± 17.68 [ac]	62.70 ± 18.18 [bc]	79.20 ± 14.62 [ac]
IAP_{200}	49.60 ± 12.99 [ac]	87.30 ± 18.54 [ac]	91.50 ± 18.42 [ac]	100.10 ± 10.76 [ac]
IAP_{100}	68.20 ± 10.30 [ac]	102.90 ± 16.88 [ac]	110.40 ± 12.77 [ac]	119.70 ± 11.29 [ac]

[a] $p < 0.01$ and [b] $p < 0.05$ as compared with intact vehicle control by THSD test; [c] $p < 0.01$ as compared with OVA control by THSD test.

3.7. Changes in Oxidative Stress and Inflammation-Related Gene Expressions in Lung Tissue

In the OVA control group, statistically significant ($p < 0.01$) increases in the mRNA expressions of genes associated with oxidative stress and inflammation were observed within the lung tissue. Notably, the expressions of NF-κB, p38 MAPK, PI3K, Akt, IL-4, and IL-5 genes were markedly increased, while the mRNA expression of the PTEN gene exhibited a significant reduction ($p < 0.01$). In contrast, the groups administered with all three doses of IAP extract displayed a significant ($p < 0.01$) and dose-dependent reduction in the mRNA expressions of NF-κB, p38 MAPK, PI3K, Akt, IL-4, and IL-5 genes within the lung tissue. Simultaneously, a significant ($p < 0.01$) and dose-dependent increase in the mRNA expression of the PTEN gene was noted. In particular, the IAP_{400} group exhibited a pattern of gene expression comparable to that observed in the DEXA-administered group, particularly with respect to the regulation of oxidative stress and inflammation-related genes (Table 3).

3.8. Histopathological Changes in Lung Tissues

In the OVA control group, notable sarcomatous lesions were evident, characterized by the thickening of the alveolar septa due to the infiltration of inflammatory cells, along with the presence of inflammatory cells within the alveoli and bronchioles. A statistically significant ($p < 0.01$) increase was observed in the average thickness of the alveolar septa, as well as in the infiltration of inflammatory cells into the alveolar and peribronchiolar regions. Moreover, there was an increase in the presence of eosinophilic leukocytes and mast cells, coinciding with a decrease in the ASA within the OVA control group. Conversely, in all three doses of IAP-extract-administered groups, a significant ($p < 0.01$) and dose-dependent increase was noted in the ASA, the average alveolar septum thickness, as well as in the infiltration of inflammatory cells within the alveolar and peribronchiolar regions. In addition, there was a dose-dependent increase in the number of eosinophilic leukocytes and mast cells. In particular, the IAP_{400} group demonstrated an inhibitory effect against OVA-induced reduction in the thickening of the alveolar

septal, the infiltration of inflammatory cells, including eosinophilic leukocytes and mast cells, and the related reduction in ASA. These findings are comparable to those observed in the DEXA-administered group (Figure 4 and Table 4).

Table 3. mRNA expressions in lung tissue of intact or OVA-induced allergic asthma mice.

Groups	Controls		Reference	Test Material—IAP Extract		
	Intact Vehicle	OVA	DEXA	400 mg/kg	200 mg/kg	100 mg/kg
IL-4	1.00 ± 0.07	9.15 ± 0.96 [a]	2.78 ± 1.04 [ab]	2.79 ± 0.58 [ab]	4.54 ± 1.18 [ab]	6.32 ± 1.31 [ab]
IL-5	1.00 ± 0.05	7.13 ± 1.20 [a]	2.10 ± 0.40 [ab]	2.12 ± 0.48 [ab]	3.40 ± 0.80 [ab]	4.28 ± 0.97 [ab]
NF-κB	1.00 ± 0.07	14.40 ± 3.47 [a]	3.21 ± 0.99 [ab]	3.25 ± 0.92 [ab]	6.07 ± 1.53 [ab]	8.24 ± 1.08 [ab]
p38 MAPK	1.00 ± 0.06	9.86 ± 2.68 [a]	2.82 ± 0.61 [ab]	2.85 ± 0.71 [ab]	3.96 ± 1.23 [ab]	5.72 ± 1.94 [ab]
PTEN	1.00 ± 0.06	0.18 ± 0.04 [a]	0.62 ± 0.16 [ab]	0.61 ± 0.10 [ab]	0.42 ± 0.09 [ab]	0.35 ± 0.09 [ab]
PI3K	1.00 ± 0.04	7.94 ± 0.77 [a]	2.61 ± 0.54 [ab]	2.65 ± 0.60 [ab]	4.05 ± 1.21 [ab]	5.13 ± 1.02 [ab]
Akt	1.00 ± 0.06	7.02 ± 1.31 [a]	2.36 ± 0.64 [ab]	2.38 ± 0.53 [ab]	3.53 ± 0.49 [ab]	4.35 ± 0.64 [ab]

[a] $p < 0.01$ compared with intact vehicle control using DT3 test; [b] $p < 0.01$ compared with OVA control using DT3 test.

Table 4. Histomorphometrical changes in lung—left lobe tissue in intact or OVA-induced allergic asthma mice.

Groups	Mean ASA (%/mm^2)	Mean Alveolar Septal Thickness (μm)	Mean IF Cell Numbers Infiltrated on BAR (cells/mm^2)	Mean CR+ Eosinophil Numbers Infiltrated on BAR (cells/mm^2)	Mean TB+ Mast Cell Numbers Infiltrated on BAR (cells/mm^2)
Controls					
Intact vehicle	87.55 ± 6.24	7.43 ± 1.74	43.80 ± 11.17	5.20 ± 2.70	2.60 ± 1.35
OVA	50.28 ± 6.90 [a]	55.23 ± 5.80 [d]	1008.00 ± 211.41 [d]	352.00 ± 78.05 [d]	20.50 ± 2.17 [a]
Reference					
DEXA	77.87 ± 7.28 [c]	18.43 ± 4.53 [de]	121.20 ± 38.16 [de]	34.40 ± 14.78 [de]	5.80 ± 2.20 [bc]
Test material groups					
IAP_{400}	77.07 ± 10.00 [bc]	18.81 ± 5.88 [de]	128.80 ± 77.59 [e]	35.00 ± 14.88 [de]	6.10 ± 1.52 [ac]
IAP_{200}	74.68 ± 6.55 [ac]	25.19 ± 4.11 [de]	377.20 ± 166.73 [de]	106.00 ± 18.60 [de]	10.00 ± 2.31 [ac]
IAP_{100}	69.02 ± 6.48 [ac]	34.31 ± 5.41 [de]	510.00 ± 134.63 [de]	195.90 ± 51.90 [de]	12.20 ± 2.74 [ac]

[a] $p < 0.01$ and [b] $p < 0.05$ compared with intact vehicle control via THSD test; [c] $p < 0.01$ compared with OVA control via THSD test; [d] $p < 0.01$ compared with intact vehicle control via DT3 test; [e] $p < 0.01$ compared with OVA control via DT3 test.

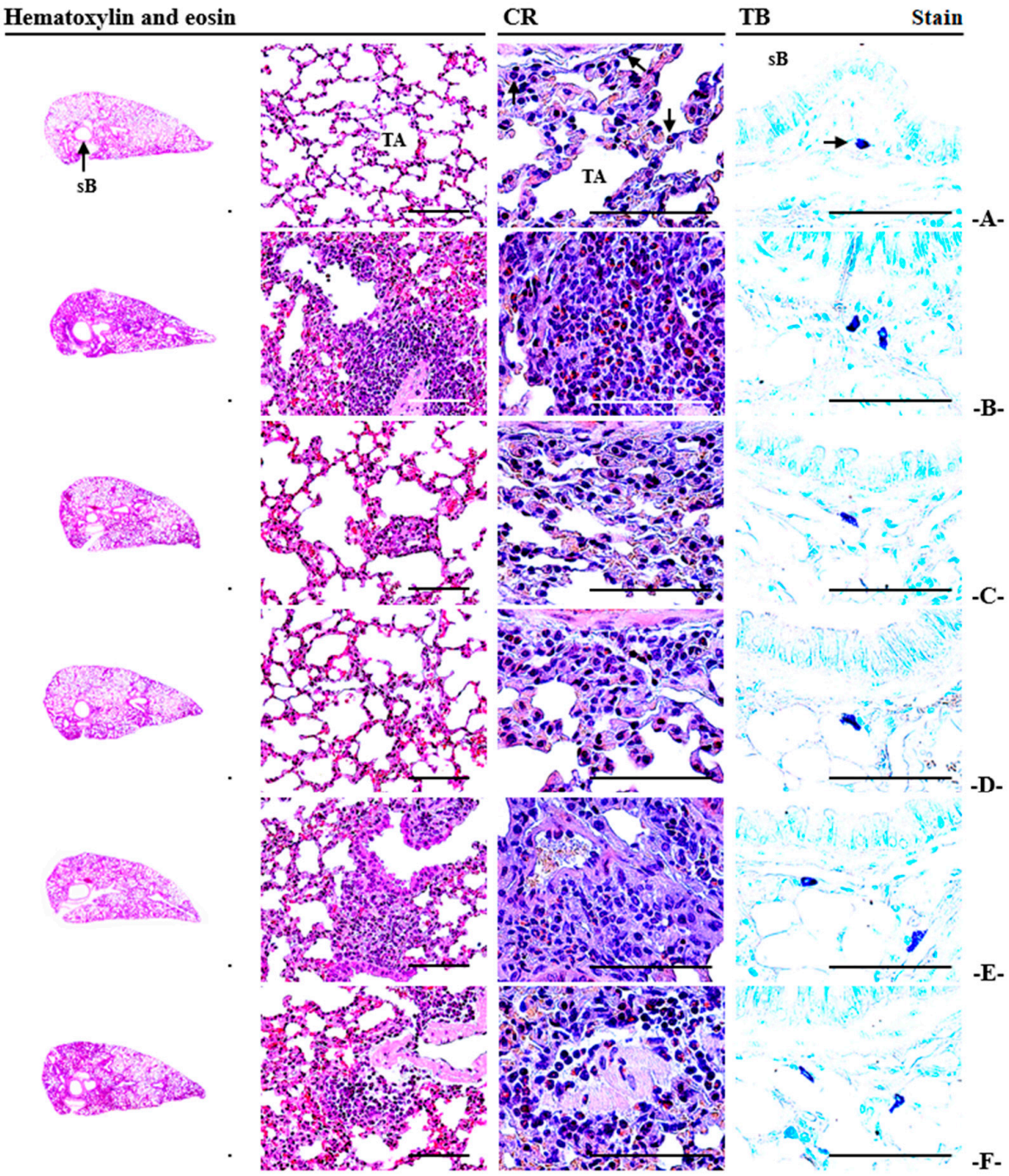

Figure 4. Representative general histopathological profiles of the lung—left lobe tissues taken from intact or OVA-induced allergic asthma mice. (**A**) Vehicle-treated normal control mice (intact vehicle control); (**B**) OVA-sensitized and boosted mice with vehicle oral administration (OVA control); (**C**) OVA-sensitized and boosted mice with oral administration of 0.75 mg/kg of DEXA (DEXA); (**D**) OVA-sensitized and boosted mice with oral administration of 400 mg/kg of IAP extract (IAP_{400}); (**E**) OVA-sensitized and boosted mice with oral administration of 200 mg/kg of IAP extract (IAP_{200}); (**F**) OVA-sensitized and boosted mice with oral administration of 100 mg/kg of IAP extract (IAP_{100}). Arrows indicate CR-positive eosinophils or TB-positive mast cells. Scale bars: 200 μm.

4. Discussion

The occurrence of significant weight loss is a recognized side effect associated with the administration of DEXA [20,21,39,51]. Similar to previous studies, the DEXA-administered group exhibited a significant decline in body weight, which commenced either 7 days or 14 days following the initiation of test substance administration. The amount of weight gain during the 16-day administration period also showed a significant decrease. This reduction in weight was statistically significant in comparison to both the intact vehicle control group and the OVA control group. In contrast, no significant variations in body weights and weight gains were observed in all three IAP-extract-administered groups. These outcomes suggest that the administration of IAP extract did not induce any significant side effects, as the changes in the body weights remained within the range of weight gain that is typically exhibited by C57BL/6 mice of the same age [52,53].

The lung weight index, which is a measure of the lung weight relative to the body weight, is a valuable parameter for assessing the pulmonary edema resulting from increased vascular leakage [21,54]. In this context of OVA-induced asthma in mice, part of the inflammatory response involves the weakening of the binding forces between vascular endothelial cells, leading to increased vascular leakage, pulmonary edema, and a subsequent increase in lung weight [55–57]. In contrast to this study, lung enlargement accompanied by noticeable local congestion, a manifestation of lung edema, was observed in the OVA-sensitized mice subjected to local re-exposure through nasal cavity injection. This was reflected in a significant increase in visual congestion, as well as in the absolute and relative lung weights, compared to the intact vehicle control group. Conversely, in comparison to the OVA control group, the groups administered with all three doses of IAP extract demonstrated significant reductions in the gross lung congestion and in both absolute and relative lung weights. These reductions occurred in a dose-dependent manner and was evident across all three doses of IAP-extract-administered groups. These results provide compelling evidence that the oral administration of IAP extract has a dose-dependent suppressive effect on OVA-induced pulmonary edema. This suppression is likely attributed to the anti-inflammatory properties of IAP extract, which result in a reduction in vascular leakage and subsequent pulmonary edema.

The observed findings align with the outcomes of previous studies using OVA-induced allergic asthma mouse models [20,21,56]. Consistent with these earlier investigations, the present study also reveals a notable increase in the total cell counts within the BALF. This increase encompasses higher counts of total leukocytes, lymphocytes, neutrophils, coral leukocytes, and monocytes. These elevated cell counts serve as markers of allergic inflammation, which is attributable to the process of OVA sensitization followed by topical re-exposure through nasal cavity injection. Conversely, significant decreases in the counts of lymphocytes, total leukocytes, total cells, neutrophils, coral leukocytes, and monocytes were noted within the BALF. These reductions exhibited a dose-dependent suppression of OVA-induced allergic inflammatory responses in the IAP-administered groups. These findings serve as indirect yet compelling evidence that the administration of IAP extract effectively curtails allergic inflammatory outcomes and re-exposure, underscoring the anti-inflammatory potential of IAP extract in the context of allergic asthma.

Allergic asthma stands as a prominent exemplar of chronic inflammatory respiratory diseases, with sustained hypersensitivity reactions derived by elevated levels of sIg E and the induction of mucus-producing goblet cell proliferation within the airway epithelium [58]. Experimental animal models of allergic asthma induced by OVA have consistently demonstrated marked increases in both the serum and BALF IgE content [18,20,21,58]. Similarly, the current study shows a significant increase in the OVA-sIg E content within the serum, representing a hallmark of the allergic inflammation triggered by OVA sensitization and subsequent nasal re-exposure. In contrast, the groups treated with various doses of IAP extract exhibited a significant decrease in the serum OVA-sIg E content in a dose-dependent manner when compared with the OVA control group. This outcome

underscores the anti-allergic inflammatory potential of IAP extract, as evidenced by its ability to suppress the OVA-induced increase in the serum OVA-sIg E content.

Th2 cells and the corresponding inflammatory cytokines play pivotal roles in the pathogenesis of allergic asthma [58,59]. In particular, IL-4 promotes the differentiation of IgE-producing B lymphocytes, thereby fostering the development of allergic inflammation and airway remodeling [11,12]. IL-5 is specifically associated with eosinophilic leukocytes, contributing to their proliferation, differentiation, migration, activity, replenishment, and survival. The differentiation of eosinophilic leukocytes within tissues is associated with the induction of various allergic reactions, including asthma [14]. This study employed an enzyme-linked immunosorbent assay (ELISA) and real-time RT-PCR analyses to ascertain the levels of IL-4 and IL-5 both in the BALF and lung tissue. The results indicate noteworthy increases in the IL-4 and IL-5 contents, alongside increased IL-4 and IL-5 mRNA expressions, following OVA sensitization and topical re-exposure through nasal administration. Conversely, the administration of various doses of IAP extract led to significant reductions in the IL-4 and IL-5 contents and in the mRNA expressions within both the BALF and lung tissue, demonstrating a dose-dependent pattern. These findings collectively provide compelling evidence that the oral administration of IAP extract effectively mitigates OVA-induced allergic asthma in a dose-dependent manner by modulating the activity of Th2-cell-associated inflammatory cytokines, especially IL-4 and IL-5.

The pathological manifestations of asthma have been primarily centered around excessive mucus production, airway obstruction, and the infiltration of various inflammatory cells including lymphocytes, eosinophilic leukocytes, and mast cells [20,21,60]. Histopathological examinations have consistently revealed significant alterations, such as the thickening of the alveolar septa due to the presence of inflammatory cells, and the infiltration of various inflammatory cells including mast cells and eosinophilic leukocytes around the alveoli and bronchioles in the lungs of allergic asthma mouse models induced by OVA sensitization and local re-exposure through nasal administration [20,21,24,56]. The assessment of the ASA (%/mm^2) serves as a critical indicator of indirect lung gas exchange capacity. A reduction in the ASA corresponds to a decline in the gas exchange surface area within the lung, resulting in diminished lung function. A decreased ASA has been histopathologically reported in different lung diseases [20,21,39,43,44,61]. In line with previous findings from drug efficacy experiments conducted on OVA-induced allergic asthma models [20,21,24,56], the current study observed significant sarcomatous lesions characterized by the thickening of the alveolar septum due to the infiltration of inflammatory cells around the alveoli and bronchioles in response to OVA sensitization and local re-exposure through nasal administration. Furthermore, a histomorphometric analysis demonstrated significant increases in the thickness of the mean alveolar septum, as well as the presence of infiltrating inflammatory cells within the alveoli and peribronchiolar regions, including eosinophilic leukocytes and mast cells. These changes were associated with a reduction in the ASA compared to the intact vehicle control group. In contrast, compared to the OVA control group, the IAP-extract-administered groups showed significant and dose-dependent increases in the ASA, the average alveolar septal thickness, infiltrating inflammatory cells within the alveoli and peribronchiolar regions, eosinophilic leukocytes, and mast cell numbers. These findings provide compelling direct evidence suggesting that the oral administration of IAP extract has the potential to suppress OVA-induced allergic asthma in a dose-dependent manner through its anti-inflammatory effects.

NF-κB, a crucial player in inflammation linked to reactive oxygen species (ROS), exerts its effects by binding to promoters encoding tumor necrosis factor (TNF)-α, ILs (IL-1 and IL-6), and certain adhesion molecules [62,63]. Moreover, NF-κB regulates the expression of various cytokines that are directly involved in the inflammatory response [64,65]. Its overexpression is well documented in allergic asthma, and the upregulation of p38 MAPK, PI3K, and Akt is also observed alongside an increase in NF-κB expression [5–7,66,67]. Furthermore, PTEN serves as a pivotal suppressor of tumorigenesis within the PI3K/Akt signaling pathway. Abnormalities in the PTEN gene contribute to the pathogenesis of

various malignancies [68–70]. PTEN gene expression is modulated by the MAPK signaling pathway [71], where inhibiting the MAPK signaling pathway substantially curtains malignant tumor development by maintaining PTEN expression [70,72]. Currently, the enhanced PTEN expression or suppression of PI3K activity has emerged as a potential strategy to alleviate allergic asthma through the regulation of various signal transduction pathways [66,73,74]. In this study, OVA sensitization and local re-exposure through nasal administration led to a significant increase in oxidative stress and inflammation-related NF-κB, p38 MAPK, PI3K, and Akt mRNA expressions, coupled with a decrease in PTEN mRNA expression within lung tissue. Conversely, a dose-dependent attenuation of oxidative stress-induced inflammatory lung damage was evident through the modulation of OVA-induced PI3K/AKT/PTEN, p38 MAPK, and NF-κB mRNA expressions in all three doses of IAP-administered groups.

The findings of this study collectively provide compelling evidence supporting the potential of the oral administration of IAP extract in the dose-dependent mitigation of OVA-induced allergic asthma, oxidative stress, and inflammatory lung damage. This effect is likely medicated through the anti-inflammatory and antioxidant activities, achieved by regulating key signaling pathways including p38 MAPK, NF-κB, and PI3K/Akt/PTEN. Nevertheless, it is important to acknowledge the several limitations of this study. Further research could delve deeper into elucidating the specific mechanisms by which IAP extract influences the PI3K-Akt pathway, possibly involving phosphorylation events, in the context of the OVA-induced in vivo asthma model. Additionally, conducting electron microscopic studies on lung tissues might offer valuable insights into the ultrastructural changes underlying the observed effects. While the present study contributes valuable insights into asthma research, it is essential to recognize that further rigorous clinical studies are necessary to corroborate these findings before considering the incorporation of Asian pear extract into health-functional foods or pharmaceutical products.

5. Conclusions

The results of this study, conducted on female C57BL/6J mice, offer compelling evidence that the allergic asthma induced by OVA sensitization and topical re-exposure in the nasal cavity can be effectively inhibited in a dose-dependent manner through the oral administration of IAP extract at concentrations ranging from 400 to 100 mg/kg. These beneficial effects are attributed to the anti-inflammatory and antioxidant activities of IAP extract, which are facilitated by the regulation of key gene expressions including PI3K/Akt/PTEN, p38 MAPK, and NF-κB. Importantly, the inhibitory impact observed in the groups administered with IAP extract at 400 mg/kg was comparable to that of the group treated with DEXA at 0.75 mg/kg. This highlights the potential of IAP extract, particularly in a higher dose, as a promising candidate for the development of a more effective natural therapeutic agent or health-functional food ingredient aimed at enhancing respiratory function. It should be emphasized, however, that while these findings are promising, further research and clinical validation are necessary to establish the safety, efficacy, and potential applications of IAP extract in addressing allergic asthma and respiratory health. This study lays a robust foundation for future endeavors in this area, signaling the potential for the development of innovative approaches to respiratory wellness utilizing natural compounds.

Supplementary Materials: The following supporting information can be downloaded at https://www.mdpi.com/article/10.3390/app13169342/s1, Figure S1: HPLC analysis of standard arbutin (A) and arbutin in IAP extract (B); Table S1: Oligonucleotides for quantitative RT-PCR analysis; Table S2: Body weight gains in intact or OVA-induced allergic asthma mice; Table S3: Lung weights and gross inspections in intact or OVA-induced allergic asthma mice.

Author Contributions: Conceptualization, K.-Y.K., S.-K.K. and J.-S.C.; methodology, K.-Y.K., S.S., E.-J.H., S.-K.K. and J.-S.C.; software, S.-K.K.; validation, K.M.I.B., J.W.K., S.-K.K. and J.-S.C.; formal analysis, M.R.K., J.-H.L., M.-U.K., J.W.K., S.S., E.-J.H. and S.-K.K.; investigation, M.R.K., K.M.I.B., J.W.K., S.-K.K. and J.-S.C.; resources, S.-K.K.; data curation, M.R.K., K.M.I.B., J.-H.L., M.-U.K., J.W.K., K.-Y.K., S.S. and E.-J.H.; writing—original draft preparation, M.R.K., K.M.I.B., S.-K.K. and J.-S.C.; writing—review and editing, K.M.I.B., S.-K.K. and J.-S.C.; visualization, K.M.I.B., J.W.K., K.-Y.K., S.S. and E.-J.H.; supervision, S.-K.K. and J.-S.C.; project administration, K.-Y.K. and S.-K.K. All authors have read and agreed to the published version of the manuscript.

Funding: This work was supported by the Korea Institute of Planning and Evaluation for Technology in Food, Agriculture, and Forestry (IPET) through the High Value-Added Food Technology Development Program, funded by the Ministry of Agriculture, Food and Rural Affairs (MAFRA; 122027-2).

Institutional Review Board Statement: This study was conducted following the national regulations of the usage and welfare of laboratory animals and was approved by the Animal Care and Use Committee of Daegu Haany University (approval no. DHU2022-120; approved on 20 December 2022).

Informed Consent Statement: Not applicable.

Data Availability Statement: Not applicable.

Conflicts of Interest: The authors declare no conflict of interest.

Abbreviations

Akt: Protein kinase B; $Al(OH)_3$: Aluminum hydroxide; ANOVA: One way analysis of variance test; ASA: Alveolar surface area; BALF: Bronchoalveolar lavage fluid; BAR: Bronchiole-alveolar region; CR: Congo red; Day-1: One day before initial test article administration; Day 10: The day of sacrifice, 24 h after last 16th test material administration; DEXA: Dexamethasone; DT3: Dunnett's T3 test; ELISA: Enzyme-linked immunosorbent assay; H&E: Hematoxylin and eosin; HPLC: High-performance liquid chromatography; IAP: Immature Asian pear extract; IF: Inflammatory; IgE: Immunoglobulin E; IL: Interleukin; IP: Intraperitoneal; KH_2PO_4: Monopotassium phosphate; MAPK: Mitogen-activated protein kinases; NF-κB: Nuclear factor kappa-light-chain-enhancer of activated B cells; OVA: Ovalbumin; p38 MAPK: p38 mitogen-activated protein kinase; pB: Primary bronchiole; PI3K: Phosphoinositide 3-kinase; PTEN: Phosphatase and TENsin homolog deleted on chromosome 10; RT-PCR: Reverse transcription polymerase chain reaction; sB: Secondary bronchus; sIg: Specific immunoglobulin; TA: Terminal respiratory bronchiole-alveoli; TB: Toluidine blue; Th2: Type 2 helper T cells; THSD: Tukey's honest significant difference test; TNF: Tumor necrosis factor.

References

1. Takeda, K.; Thurman, J.M.; Tomlinson, S.; Okamoto, M.; Shiraishi, Y.; Ferreira, V.P.; Cortes, C.; Pangburn, M.K.; Holers, V.M.; Gelfand, E.W. The critical role of complement alternative pathway regulator factor H in allergen-induced airway hyperresponsiveness and inflammation. *J. Immunol.* **2012**, *188*, 661–667. [CrossRef]
2. Holgate, S.T. The airway epithelium is central to the pathogenesis of asthma. *Allergol. Int.* **2008**, *57*, 1–10. [CrossRef] [PubMed]
3. Bochner, B.S.; Rothenberg, M.E.; Boyce, J.A.; Finkelman, F. Advances in mechanisms of allergy and clinical immunology in 2012. *J. Allergy Clin. Immunol.* **2013**, *131*, 661–667. [CrossRef]
4. Braman, S.S. The global burden of asthma. *Chest* **2006**, *130*, 4S–12S. [CrossRef]
5. Li, Y.; Chen, S.; Chi, Y.; Yang, Y.; Chen, X.; Wang, H.; Lv, Z.; Wang, J.; Yuan, L.; Huang, P.; et al. Kinetics of the accumulation of group 2 innate lymphoid cells in IL-33-induced and IL-25-induced murine models of asthma: A potential role for the chemokine CXCL16. *Cell. Mol. Immunol.* **2019**, *16*, 75–86. [CrossRef] [PubMed]
6. Song, Y.; Wang, Z.; Jiang, J.; Piao, Y.; Li, L.; Xu, C.; Piao, H.; Li, L.; Yan, G. DEK-targeting aptamer DTA-64 attenuates bronchial EMT-mediated airway remodeling by suppressing TGF-β1/Smad, MAPK and PI3K signaling pathway in asthma. *J. Cell. Mol. Med.* **2020**, *24*, 13739–13750. [CrossRef]

7. Tirpude, N.V.; Sharma, A.; Joshi, R.; Kumari, M.; Acharya, V. Vitex negundo Linn. extract alleviates inflammatory aggravation and lung injury by modulating AMPK/PI3K/Akt/p38-NF-κB and TGF-β/Smad/Bcl2/caspase/LC3 cascade and macrophages activation in murine model of OVA-LPS induced allergic asthma. *J. Ethnopharmacol.* **2021**, *271*, 113894. [CrossRef]
8. Liu, X.; Yu, D.; Wang, T. Sappanone A attenuates allergic airway inflammation in ovalbumin-induced asthma. *Int. Arch. Allergy Immunol.* **2016**, *170*, 180–186. [CrossRef]
9. Liang, P.; Peng, S.; Zhang, M.; Ma, Y.; Zhen, X.; Li, H. Huai Qi Huang corrects the balance of Th1/Th2 and Treg/Th17 in an ovalbumin-induced asthma mouse model. *Biosci. Rep.* **2017**, *37*, BSR20171071. [CrossRef] [PubMed]
10. Venturini, C.L.; Macho, A.; Arunachalam, K.; de Almeida, D.A.T.; Rosa, S.I.G.; Pavan, E.; Balogun, S.O.; Damazo, A.S.; Martins, D.T.O. Vitexin inhibits inflammation in murine ovalbumin-induced allergic asthma. *Biomed. Pharmacother.* **2018**, *97*, 143–151. [CrossRef]
11. Jie, Z.; Jin, M.; Cai, Y.; Bai, C.; Shen, Y.; Yuan, Z.; Hu, Y.; Holgate, S. The effects of Th2 cytokines on the expression of ADAM33 in allergen-induced chronic airway inflammation. *Respir. Physiol. Neurobiol.* **2009**, *168*, 289–294. [CrossRef]
12. Deo, S.S.; Mistry, K.J.; Kakade, A.M.; Niphadkar, P.V. Role played by Th2 type cytokines in IgE mediated allergy and asthma. *Lung India* **2010**, *27*, 66–71. [CrossRef]
13. Simon, D.; Braathen, L.R.; Simon, H.U. Eosinophils and atopic dermatitis. *Allergy* **2004**, *59*, 561–570. [CrossRef]
14. Cameron, L.; Christodoulopoulos, P.; Lavigne, F.; Nakamura, Y.; Eidelman, D.; McEuen, A.; Walls, A.; Tavernier, J.; Minshall, E.; Moqbel, R.; et al. Evidence for local eosinophil differentiation within allergic nasal mucosa: Inhibition with soluble IL-5 receptor. *J. Immunol.* **2000**, *164*, 1538–1545. [CrossRef] [PubMed]
15. Rana, S.; Shahzad, M.; Shabbir, A. *Pistacia integerrima* ameliorates airway inflammation by attenuation of TNF-α, IL-4, and IL-5 expression levels, and pulmonary edema by elevation of AQP1 and AQP5 expression levels in mouse model of ovalbumin-induced allergic asthma. *Phytomedicine* **2016**, *23*, 838–845. [CrossRef]
16. Inam, A.; Shahzad, M.; Shabbir, A.; Shahid, H.; Shahid, K.; Javeed, A. *Carica papaya* ameliorates allergic asthma via down regulation of IL-4, IL-5, eotaxin, TNF-α, NF-κB, and iNOS levels. *Phytomedicine* **2017**, *32*, 1–7. [CrossRef] [PubMed]
17. Choi, M.S.; Park, S.; Choi, T.; Lee, G.; Haam, K.K.; Hong, M.C.; Min, B.I.; Bae, H. Bee venom ameliorates ovalbumin induced allergic asthma via modulating CD4 + CD25+ regulatory T cells in mice. *Cytokine* **2013**, *61*, 256–265. [CrossRef] [PubMed]
18. Habibian, R.; Delirezh, N.; Farshid, A.A. The effects of bone marrow-derived mesenchymal stem cells on ovalbumin-induced allergic asthma and cytokine responses in mice. *Iran. J. Basic Med. Sci.* **2018**, *21*, 483–488. [PubMed]
19. Kwon, O.K.; Ahn, K.S.; Lee, M.Y.; Kim, S.Y.; Park, B.Y.; Kim, M.K.; Lee, I.Y.; Oh, S.R.; Lee, H.K. Inhibitory effect of kefiran on ovalbumin-induced lung inflammation in a murine model of asthma. *Arch. Pharm. Res.* **2008**, *31*, 1590–1596. [CrossRef]
20. Ku, S.K.; Kim, J.W.; Cho, H.R.; Kim, K.Y.; Min, Y.H.; Park, J.H.; Kim, J.S.; Park, J.H.; Seo, B.I.; Roh, S.S. Effect of β-glucan originated from *Aureobasidium pullulans* on asthma induced by ovalbumin in mouse. *Arch. Pharm. Res.* **2012**, *35*, 1073–1081. [CrossRef]
21. Min, B.G.; Park, S.M.; Choi, Y.W.; Ku, S.K.; Cho, I.J.; Kim, Y.W.; Byun, S.H.; Park, C.A.; Park, S.J.; Na, M.; et al. Effects of *Pelargonium sidoides* and *Coptis rhizoma* 2 : 1 mixed formula (PS + CR) on ovalbumin-induced asthma in mice. *eCAM* **2020**, *2020*, 9135637. [CrossRef] [PubMed]
22. Piao, C.H.; Fan, Y.J.; Nguyen, T.V.; Song, C.H.; Chai, O.H. Mangiferin alleviates ovalbumin-induced allergic rhinitis via Nrf2/HO-1/NF-κB signaling pathways. *Int. J. Mol. Sci.* **2020**, *21*, 3415. [CrossRef]
23. Wang, P.; Liu, H.; Fan, X.; Zhu, Z.; Zhu, Y. Effect of San'ao decoction on aggravated asthma mice model induced by $PM_{2.5}$ and TRPA1/TRPV1 expressions. *J. Ethnopharmacol.* **2019**, *236*, 82–90. [CrossRef] [PubMed]
24. André, D.M.; Horimoto, C.M.; Calixto, M.C.; Alexandre, E.C.; Antunes, E. Epigallocatechin-3-gallate protects against the exacerbation of allergic eosinophilic inflammation associated with obesity in mice. *Int. Immunopharmacol.* **2018**, *62*, 212–219. [CrossRef]
25. Devipriya, D.; Gowri, S.; Nideesh, T.R. Hepatoprotective effect of *Pterocarpus marsupium* against carbon tetrachloride induced damage in albino rats. *Anc. Sci. Life* **2007**, *27*, 19–25. [PubMed]
26. Kim, H.S.; Park, S.I.; Choi, S.H.; Song, C.H.; Park, S.J.; Shin, Y.K.; Han, C.H.; Lee, Y.J.; Ku, S.K. Single oral dose toxicity test of blue honeysuckle concentrate in mice. *Toxicol. Res.* **2015**, *31*, 61–68. [CrossRef]
27. Lin, L.Z.; Harnly, J.M. Phenolic compounds and chromatographic profiles of pear skins (*Pyrus* spp.). *J. Agric. Food Chem.* **2008**, *56*, 9094–9101. [CrossRef] [PubMed]
28. Lee, K.H.; Cho, J.Y.; Lee, H.J.; Ma, Y.K.; Kwon, J.; Park, S.H.; Lee, S.H.; Cho, J.A.; Kim, W.S.; Park, K.H.; et al. Hydroxycinnamoylmalic acids and their methyl esters from pear (*Pyrus pyrifolia* Nakai) fruit peel. *J. Agric. Food Chem.* **2011**, *59*, 10124–10128. [CrossRef]
29. Cho, J.Y.; Kim, C.H.; Lee, H.J.; Lee, S.H.; Cho, J.A.; Kim, W.S.; Park, K.H.; Moon, J.H. Caffeoyl triterpenes from pear (*Pyrus pyrifolia* Nakai) fruit peels and their antioxidative activities against oxidation of rat blood plasma. *J. Agric. Food Chem.* **2013**, *61*, 4563–4569. [CrossRef]
30. Lee, K.H.; Cho, J.Y.; Lee, H.J.; Park, K.Y.; Ma, Y.K.; Lee, S.H.; Cho, J.A.; Kim, W.S.; Park, K.H.; Moon, J.H. Isolation and identification of phenolic compounds from an Asian pear (*Pyrus pyrifolia* Nakai) fruit peel. *Food Sci. Biotechnol.* **2011**, *20*, 1539–1545. [CrossRef]
31. Lee, Y.G.; Cho, J.Y.; Kim, C.M.; Jeong, H.Y.; Lee, D.I.; Kim, S.R.; Lee, S.H.; Kim, W.S.; Park, K.H.; Moon, J.H. Isolation and identification of 3 low-molecular compounds from pear (*Pyrus pyrifolia* Nakai cv. Chuhwangbae) fruit peel. *Korean J. Food Sci. Technol.* **2013**, *45*, 174–179. [CrossRef]

32. Lee, Y.G.; Cho, J.Y.; Kim, C.M.; Lee, S.H.; Kim, W.S.; Jeon, T.I.; Park, K.H.; Moon, J.H. Coumaroyl quinic acid derivatives and flavonoids from immature pear (*Pyrus pyrifolia* Nakai) fruit. *Food Sci. Biotechnol.* **2013**, *22*, 803–810. [CrossRef]
33. Cho, J.Y.; Lee, Y.G.; Lee, S.H.; Kim, W.S.; Park, K.H.; Moon, J.H. An ether and three ester derivatives of phenylpropanoid from pear (*Pyrus pyrifolia Nakai* cv. Chuhwangbae) fruit and their radical-scavenging activity. *Food Sci. Biotechnol.* **2014**, *23*, 253–259. [CrossRef]
34. Cho, J.Y.; Kim, E.H.; Yun, H.R.; Jeong, H.Y.; Lee, Y.G.; Kim, W.S.; Moon, J.H. Change in chemical constituents and free radical-scavenging activity during pear (*Pyrus pyrifolia*) cultivar fruit development. *Biosci. Biotechnol. Bioch.* **2015**, *79*, 260–270. [CrossRef] [PubMed]
35. Lee, S.W.; Cho, J.Y.; Jeong, H.Y.; Na, T.W.; Lee, S.H.; Moon, J.H. Enhancement of antioxidative and antimicrobial activities of immature pear (*Pyrus pyrifolia* cv. Niitaka) fruits by fermentation with *Leuconostoc mesenteroides*. *Food Sci. Biotechnol.* **2016**, *25*, 1719–1726. [CrossRef] [PubMed]
36. Cho, J.Y.; Park, K.Y.; Lee, K.H.; Lee, H.J.; Lee, S.H.; Cho, J.A.; Kim, W.S.; Shin, S.C.; Park, K.H.; Moon, J.H. Recovery of arbutin in high purity from fruit peels of pear (*Pyrus pyrifolia* Nakai). *Food Sci. Biotechnol.* **2011**, *20*, 801–807. [CrossRef]
37. Lee, H.S.; Isse, T.; Kawamoto, T.; Woo, H.S.; Kim, A.K.; Park, J.Y.; Yang, M. Effects and action mechanisms of Korean pear (*Pyrus pyrifolia* cv. Shingo) on alcohol detoxification. *Phytother. Res.* **2012**, *26*, 1753–1758. [CrossRef]
38. Lee, H.S.; Isse, T.; Kawamoto, T.; Baik, H.W.; Park, J.Y.; Yang, M. Effect of Korean pear (*Pyrus pyrifolia* cv. Shingo) juice on hangover severity following alcohol consumption. *Food Chem. Toxicol.* **2013**, *58*, 101–106. [CrossRef]
39. Park, S.M.; Jung, C.J.; Lee, D.G.; Choi, B.R.; Ku, T.H.; La, I.J.; Cho, I.J.; Ku, S.K. *Adenophora stricta* root extract protects lung injury from exposure to particulate matter 2.5 in mice. *Antioxidants* **2022**, *11*, 1376. [CrossRef]
40. Negara, B.F.S.P.; Kim, J.W.; Bashir, K.M.I.; Lee, J.H.; Ku, M.U.; Kim, K.Y.; Shin, S.; Hong, E.J.; Ku, S.K.; Choi, J.S. Expectorant effects of immature Asian pear extract on $PM_{2.5}$-induced subacute pulmonary injury in mice. *J. Food Biochem.* **2023**, *2023*, 5671679. [CrossRef]
41. Chen, Y.; Xi, Y.; Li, M.; Wu, Y.; Yan, W.; Dai, J.; Wu, M.; Ding, W.; Zhang, J.; Zhang, F.; et al. Maternal exposure to $PM_{2.5}$ decreases ovarian reserve in neonatal offspring mice through activating PI3K/AKT/FoxO3a pathway and ROS-dependent NF-κB pathway. *Toxicology* **2022**, *481*, 153352. [CrossRef]
42. Guo, Y.; Cao, Z.; Jiao, X.; Bai, D.; Zhang, Y.; Hua, J.; Liu, W.; Teng, X. Pre-pregnancy exposure to fine particulate matter ($PM_{2.5}$) increases reactive oxygen species production in oocytes and decrease litter size and weight in mice. *Environ. Pollut.* **2021**, *268*, 115858. [CrossRef]
43. Hu, J.R.; Jung, C.J.; Ku, S.M.; Jung, D.H.; Ku, S.K.; Choi, J.-S. Antitussive, expectorant, and anti-inflammatory effects of Adenophorae Radix powder in ICR mice. *J. Ethnopharmacol.* **2019**, *239*, 111915. [CrossRef] [PubMed]
44. Hu, J.R.; Jung, C.J.; Ku, S.M.; Jung, D.H.; Bashir, K.M.I.; Ku, S.-K.; Choi, J.-S. Anti-inflammatory, expectorant, and antitussive properties of Kyeongok-go in ICR mice. *Pharm. Biol.* **2021**, *59*, 321–334. [CrossRef]
45. Bashir, K.M.I.; Kim, J.W.; Kim, J.-K.; Chun, Y.-S.; Choi, J.-S.; Ku, S.-K. Efficacy confirmation test of black cumin (*Nigella sativa* L.) seeds extract using a high-fat diet mouse model. *Metabolites* **2023**, *13*, 501. [CrossRef] [PubMed]
46. Glynos, C.; Bibli, S.I.; Katsaounou, P.; Pavlidou, A.; Magkou, C.; Karavana, V.; Topouzis, S.; Kalomenidis, I.; Zakynthinos, S.; Papapetropoulos, A. Comparison of the effects of e-cigarette vapor with cigarette smoke on lung function and inflammation in mice. *Am. J. Physiol. Lung Cell. Mol. Physiol.* **2018**, *315*, L662–L672. [CrossRef] [PubMed]
47. Shu, J.; Li, D.; Ouyang, H.; Huang, J.; Long, Z.; Liang, Z.; Chen, Y.; Chen, Y.; Zheng, Q.; Kuang, M.; et al. Comparison and evaluation of two different methods to establish the cigarette smoke exposure mouse model of COPD. *Sci. Rep.* **2017**, *7*, 15454. [CrossRef]
48. Deng, X.; Rui, W.; Zhang, F.; Ding, W. $PM_{2.5}$ induces Nrf2-mediated defense mechanisms against oxidative stress by activating PIK3/AKT signaling pathway in human lung alveolar epithelial A549 cells. *Cell Biol. Toxicol.* **2013**, *29*, 143–157. [CrossRef]
49. Duong, C.; Seow, H.J.; Bozinovski, S.; Crack, P.J.; Anderson, G.P.; Vlahos, R. Glutathione peroxidase-1 protects against cigarette smoke-induced lung inflammation in mice. *Am. J. Physiol. Lung Cell. Mol. Physiol.* **2010**, *299*, L425–L433. [CrossRef]
50. Schmittgen, T.; Livak, K. Analyzing real-time PCR data by the comparative CT method. *Nat. Protoc.* **2008**, *3*, 1101–1108. [CrossRef]
51. Piper, S.L.; Laron, D.; Manzano, G.; Pattnaik, T.; Liu, X.; Kim, H.T.; Feeley, B.T. A comparison of lidocaine, ropivacaine and dexamethasone toxicity on bovine tenocytes in culture. *J. Bone Jt. Surg. Br.* **2012**, *94*, 856–862. [CrossRef]
52. Fox, J.G.; Cohen, B.J.; Loew, F.M. *Laboratory Animal Medicine*; Academic Press Inc.: Orlando, FL, USA, 1984.
53. Tajima, Y. *Biological Reference Data Book on Experimental Animals*; Soft Science Inc.: Tokyo, Japan, 1989.
54. Tumes, D.J.; Cormie, J.; Calvert, M.G.; Stewart, K.; Nassenstein, C.; Braun, A.; Foster, P.S.; Dent, L.A. Strain-dependent resistance to allergen-induced lung pathophysiology in mice correlates with rate of apoptosis of lung-derived eosinophils. *J. Leukoc. Biol.* **2007**, *81*, 1362–1373. [CrossRef]
55. Okada, S.; Kita, H.; George, T.J.; Gleich, G.J.; Leiferman, K.M. Migration of eosinophils through basement membrane components in vitro: Role of matrix metalloproteinase-9. *Am. J. Respir. Cell Mol. Biol.* **1997**, *17*, 519–528. [CrossRef]
56. Abdelaziz, R.R.; Elmahdy, M.K.; Suddek, G.M. Flavocoxid attenuates airway inflammation in ovalbumin-induced mouse asthma model. *Chem. Biol. Interact.* **2018**, *292*, 15–23. [CrossRef] [PubMed]
57. Tillie-Leblond, I.; Gosset, P.; Le Berre, R.; Janin, A.; Prangère, T.; Tonnel, A.B.; Guery, B.P. Keratinocyte growth factor improves alterations of lung permeability and bronchial epithelium in allergic rats. *Eur. Respir. J.* **2007**, *30*, 31–39. [CrossRef] [PubMed]

58. Chu, X.; Wei, M.; Yang, X.; Cao, Q.; Xie, X.; Guan, M.; Wang, D.; Deng, X. Effects of an anthraquinone derivative from *Rheum officinale* Baill, emodin, on airway responses in a murine model of asthma. *Food Chem. Toxicol.* **2012**, *50*, 2368–2375. [CrossRef]
59. Barnes, P.J. The cytokine network in asthma and chronic obstructive pulmonary disease. *J. Clin. Investig.* **2008**, *118*, 3546–3556. [CrossRef] [PubMed]
60. Busse, W.W.; Calhoun, W.F.; Sedgwick, J.D. Mechanism of airway inflammation in asthma. *Am. Rev. Respir. Dis.* **1993**, *147*, S20–S24. [CrossRef]
61. Choi, H.Y.; Jung, T.Y.; Ku, S.-K.; Yang, H.B.; Lee, H.S. Toxico-pathological study of p,p-DDE after experimental aerosol exposed to ICR Mouse. *Toxicol. Res.* **2005**, *21*, 151–160.
62. Ribbons, K.A.; Thompson, J.H.; Liu, X.; Pennline, K.; Clark, D.A.; Miller, M.J. Anti-inflammatory properties of interleukin-10 administration in hapten-induced colitis. *Eur. J. Pharmacol.* **1997**, *323*, 245–254. [CrossRef]
63. Carini, M.; Aldini, G.; Piccone, M.; Facino, R.M. Fluorescent probes as markers of oxidative stress in keratinocyte cell lines following UVB exposure. *Farmaco* **2000**, *55*, 526–534. [CrossRef] [PubMed]
64. Lawrence, T. The nuclear factor NF-kappaB pathway in inflammation. *Cold Spring Harb. Perspect. Biol.* **2009**, *1*, a001651. [CrossRef] [PubMed]
65. Liu, T.; Zhang, L.; Joo, D.; Sun, S.C. NF-κB signaling in inflammation. *Signal Transduct. Target. Ther.* **2017**, *2*, 17023. [CrossRef]
66. Jang, H.Y.; Kwon, O.K.; Oh, S.R.; Lee, H.K.; Ahn, K.S.; Chin, Y.W. Mangosteen xanthones mitigate ovalbumin-induced airway inflammation in a mouse model of asthma. *Food Chem. Toxicol.* **2012**, *50*, 4042–4050. [CrossRef]
67. Tirpude, N.V.; Sharma, A.; Kumari, M.; Bhardwaj, N. Vitexin restores lung homeostasis by targeting vicious loop between inflammatory aggravation and autophagy mediated via multiple redox cascade and myeloid cells alteration in experimental allergic asthma. *Phytomedicine* **2022**, *96*, 153902. [CrossRef] [PubMed]
68. Zheng, H.; Ying, H.; Yan, H.; Kimmelman, A.C.; Hiller, D.J.; Chen, A.J.; Perry, S.R.; Tonon, G.; Chu, G.C.; Ding, Z.; et al. p53 and Pten control neural and glioma stem/progenitor cell renewal and differentiation. *Nature* **2008**, *455*, 1129–1133. [CrossRef]
69. Qi, Q.; Ling, Y.; Zhu, M.; Zhou, L.; Wan, M.; Bao, Y.; Liu, Y. Promoter region methylation and loss of protein expression of PTEN and significance in cervical cancer. *Biomed. Rep.* **2014**, *2*, 653–658. [CrossRef]
70. Li, Z.H.; Li, L.; Kang, L.P.; Wang, Y. MicroRNA-92a promotes tumor growth and suppresses immune function through activation of MAPK/ERK signaling pathway by inhibiting PTEN in mice bearing U14 cervical cancer. *Cancer Med.* **2018**, *7*, 3118–3131. [CrossRef]
71. Jiang, X.; Li, H. Overexpression of LRIG1 regulates PTEN via MAPK/MEK signaling pathway in esophageal squamous cell carcinoma. *Exp. Ther. Med.* **2016**, *12*, 2045–2052. [CrossRef]
72. Ebbesen, S.H.; Scaltriti, M.; Bialucha, C.U.; Morse, N.; Kastenhuber, E.R.; Wen, H.Y.; Dow, L.E.; Baselga, J.; Lowe, S.W. Pten loss promotes MAPK pathway dependency in HER2/neu breast carcinomas. *Proc. Natl. Acad. Sci. USA* **2016**, *113*, 3030–3035. [CrossRef]
73. Kwak, Y.G.; Song, C.H.; Yi, H.K.; Hwang, P.H.; Kim, J.S.; Lee, K.S.; Lee, Y.C. Involvement of PTEN in airway hyperresponsiveness and inflammation in bronchial asthma. *J. Clin. Investig.* **2003**, *111*, 1083–1092. [CrossRef] [PubMed]
74. Ni, Z.; Tang, J.; Cai, Z.; Yang, W.; Zhang, L.; Chen, Q.; Zhang, L.; Wang, X. A new pathway of glucocorticoid action for asthma treatment through the regulation of PTEN expression. *Respir. Res.* **2011**, *12*, 47. [CrossRef] [PubMed]